ACS ES&T Air

Open Access

pubs.acs.org/estair

Article

Elevated Environmental Lead Concentrations Following a Major Urban Fire

Published as part of ACS ES&T Air special issue "The 2025 Los Angeles Fires".

Sam J. Silva,* Seth G. John, A. Joshua West, Mia Bradshaw, Yadan Hu, Cecilia M. John, Kyeong Pil Kong, Catherine Odendahl, Nataly Pineda, Adam Ross, Brian Schlaff, Nismata Sigdel, and Katherine Thomas

Cite This: *ACS EST Air* 2026, 3, 1789–1796

Read Online

ACCESS | Metrics & More | Article Recommendations | Supporting Information

ABSTRACT: The Eaton Canyon firestorm burned thousands of acres of urban land, devastating local communities and destroying nearly 20,000 structures. Measurements of roadside dust, stormwater runoff, and atmospheric aerosols show that this fire was a source of lead (Pb) into the urban environment. Lead concentrations in roadside dust within the urban burn scar were significantly elevated immediately after the fire, remaining high through repeat rainfall events but decreasing over the course of subsequent months. During active structure fires, high aerosol lead was observed in the smoke plume. Lead in roadside rainwater was elevated in the urban burn area after the first rain. The source of lead in all cases is likely burning structures, which contained lead in paint and plumbing, resulting in widespread urban lead concentrations in excess of healthy thresholds set by regulators.

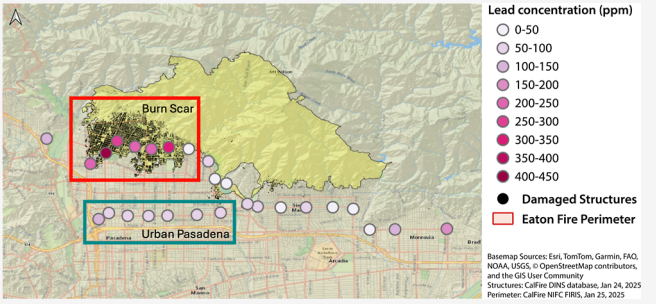

KEYWORDS: *wildfire, urban pollution, heavy metals, roadside dust, wildland–urban interface*

INTRODUCTION

Lead (Pb) is a neurotoxic heavy metal that occurs naturally in the Earth's crust. Exposure to elevated lead concentrations in humans can lead to a variety of deleterious health effects, including behavioral and learning problems in children, impacts on fetal development in pregnant women, and, if acute exposure is high enough, death.[1−3] Prior to the adoption of environmental regulations in the mid-1900s, lead was used widely—often as an additive in metal alloys, gasoline, and paints.[2,4] Lead persists in the environment, and thus, a legacy of lead contamination is still present in many urban areas. Cleanup of this legacy lead is a target of ongoing environmental remediation efforts, and the deleterious health effects of this lead are well documented and continue into the present day.[5−7]

Many buildings constructed prior to extensive environmental regulation (generally pre-1978 in the United States)[4,8] contain lead in paint and plumbing. While hazardous, this lead can often be managed such that it does not necessarily always pose an immediate public health threat. However, it can be re-exposed as older buildings degrade or are destroyed, with fire being a particularly effective pathway for releasing lead into the local environment.[9]

The Eaton Canyon firestorm was one of three major fires that burned in the greater Los Angeles, CA, area in January 2025.[10,11] The Eaton Canyon fire started on January 7th, 2025 near the city of Altadena, CA, and was not fully contained until January 31st, 2025. Driven in part by Santa Ana wind gusts reaching 100 mph, this firestorm proceeded to burn a combined 14,000 acres of forested and urban land and damaged or destroyed 19,500 structures across the cities of Altadena, Pasadena, and Sierra Madre, CA[10] (Figure 1).

In the aftermath of the Eaton Canyon fire, we collected samples to evaluate the impact on lead contamination in the environment. We investigated lead concentrations in roadside dust, atmospheric aerosol, and stormwater runoff to constrain the spatial and temporal distribution of this urban lead. We demonstrate that the Eaton Canyon fire was a source of lead far above background levels and showed that this elevated lead persisted for months.

Received: January 11, 2026
Revised: May 19, 2026
Accepted: May 21, 2026
Published: June 18, 2026

https://doi.org/10.1021/acsestair.6c00015
ACS EST Air 2026, 3, 1789–1796

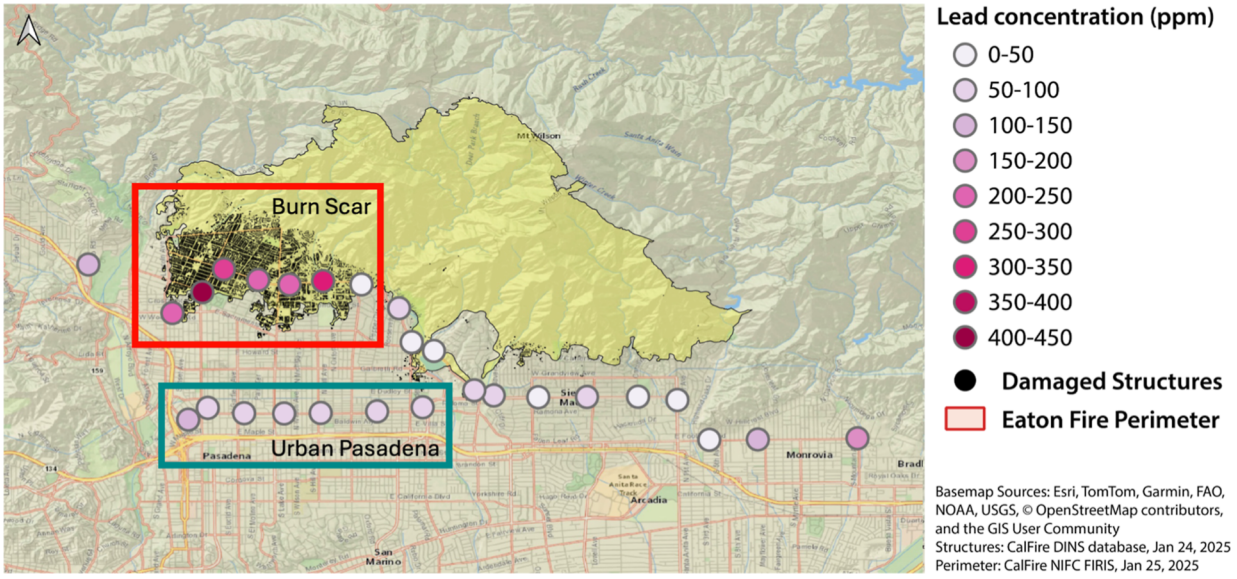

Figure 1. Area of the Eaton Canyon firestorm, with the yellow shaded region depicting the fire perimeter, and black points representing destroyed structures. Roadside dust sampling sites are shown as circles, colored by lead concentration. The red rectangle highlights the sites within the urban burn scar. The blue rectangle highlights those downwind of the fire in urban Pasadena. All other regions are coded as "foothills" and are outside of the urban burn.

MATERIALS AND METHODS

Dust was sampled from street gutters across the study area using a plastic broom and dustpan. Samples were collected in places where significant dust was present at each location, if possible compositing material from multiple sites within a few meters of the collection site. Specific coverage for each sample was dictated in part by the need to collect material of sufficient size for analysis. Many samples contained significant additional debris such as leaves, twigs, and, in some cases, litter. Samples were collected into sealed 1-gallon plastic bags, returned to the laboratory, air-dried inside their collection bags, and then sieved to isolate the fraction <250 μm using brass test sieves. This size fraction was chosen to represent the environmentally mobile material on streets.

The sieved sample was loaded into plastic XRF analysis cups (3.1 cm diameter Chemplex cups) and covered with a mylar film (3.6 mm thickness). Sample cups were filled to a standard fill level providing >2 mm thickness of the sample. Tests with differing fill amounts showed that analyzed concentrations did not depend on fill depth. Analysis was conducted using an Olympus Vanta Core portable X-ray Fluorescence analyzer (pXRF). Although this unit is capable of hand-held use and use in the field, data reported here are from analysis with the unit mounted inside a Vanta laboratory workstation, converting it to a "benchtop" function and minimizing variability in sample position. The analyzer uses a 4 W X-ray tube and a silicon drift detector and was employed with its 8–40 kV W anode for the reported Pb analyses. Analysis was conducted with collimation to a 3 mm diameter beam spot size, effectively representing the area of the sample surface over which the analysis was conducted.

The use of pXRF for determination of Pb contents in urban soils is well established in the scientific literature.[38] Accuracy and precision are generally highest when using ex situ methods (e.g., in a laboratory setting) such as those adopted here, including drying to mitigate the effects of moisture content, use of a uniform grain size, and preparation of samples in measurement cups.[39] Under such conditions, pXRF analyses can yield data that are statistically indistinguishable from methods using inductively coupled plasma mass spectrometry (ICP–MS) that are typically regulatory standard.[40]

The nominal detection limit for Pb using the Vanta Core is reported by the manufacturer as 5 ppm, though in practice with the methods used, the limit of quantitation was found to be approximately 20 ppm. Analysis of 6 certified reference materials (CRMs) following this method during the timespan of sample analyses yielded median accuracy relative to certified values ranging from 1.9% (for NIST 1633) to 41.3% (for TILL-1, a less well-characterized reference material that also yielded many values below the detection limit). The median for the three NIST reference materials was all within 5% of certified values (Figure S1), and mean values were within 2.5%. The reproducibility of CRM analyses, reported as % relative standard deviation (% RSD) of all CRM analyses, ranged from 5.6% (for NIST 2587) to 56.1% (for TILL-1) and was inversely related to Pb content. Deviation over time in CRM analyses was approximately random. Results from CRM analyses are shown in Figure S1. The % RSD on soil sample Pb analyses via this method (triplicates, n = 38 performed during the same period of time as the sample analyses) ranged from 4.5 to 72.5%, with a median of 19.5% and no relationship with concentration.

Street runoff samples were collected on January 26th at the same sites where dust samples had been collected the day before. Rainfall had started the night of January 25th and continued into the morning of January 26th, delivering a total of 0.6 in. precipitation. Samples were collected near the end of the rainfall from water flowing or standing in street gutters. Samples were collected directly from the gutters in polyethylene bags and transported back to the laboratory, where they were filtered and acidified with 0.1% trace-clean hydrochloric acid. Samples were then diluted 10-fold in 1.4 N nitric acid spiked with 10 ppb In and analyzed using an Agilent 8900 Triple Quad ICP–MS. The instrument was tuned to achieve the highest sensitivities for ^{57}Fe, ^{115}In, and ^{208}Pb in a 10 ppb multielement standard under MS/MS mode without using collision gas by using the autotune function of the MassHunter Workstation. As the sensitivities were optimized, 2.0–2.5 mL min^{-1} H_2 gas was introduced into the collision cell of the ICP–MS to reduce the isobaric interferences on the elements of interest. The samples and multielement standard solutions containing 10, 100, and 1000 ng g^{-1} Li, Be, B, Na, Mg, Al, Si, P, S, K, Ca, Ti, V, Cr, Mn, Fe, Co, Ni, Cu, Zn, As, Se, Sr, Mo, Cd, Sn, Sb, Ba, Pb, and In then were measured for their ^{7}Li, ^{9}Be, ^{11}B, ^{23}Na, ^{24}Mg, ^{27}Al, ^{28}Si, ^{31}P, ^{34}S, ^{39}K, ^{44}Ca, ^{49}Ti, ^{51}V, ^{52}Cr, ^{55}Mn, ^{56}Fe, ^{59}Co, ^{60}Ni, ^{65}Cu, ^{66}Zn, ^{75}As, ^{78}Se, ^{88}Sr, ^{95}Mo, ^{110}Cd, ^{117}Sn, ^{121}Sb, ^{137}Ba, ^{208}Pb, and ^{115}In signals under the MS/MS H_2 mode. The samples' elemental composition was obtained by calibrating with In internally and with the multielement standards externally.

https://doi.org/10.1021/acsestair.6c00015
ACS EST Air 2026, 3, 1789–1796

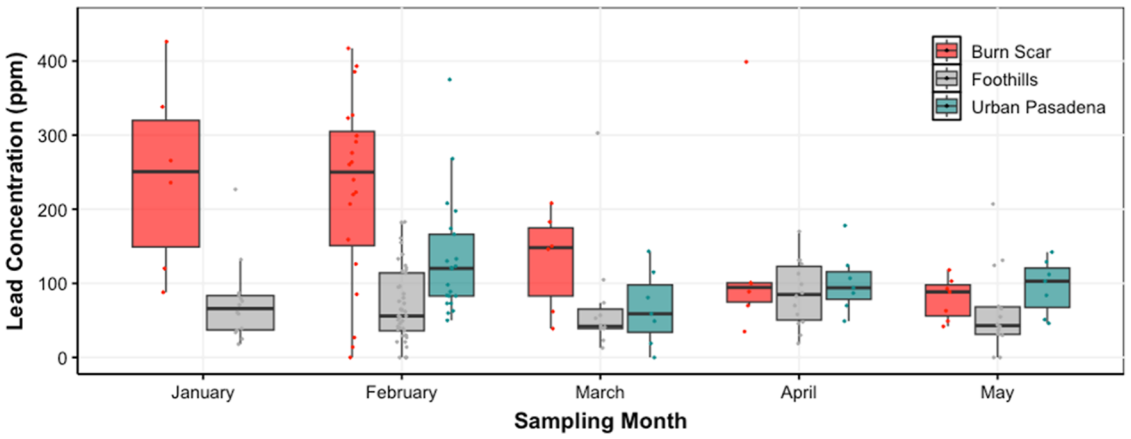

Figure 2. Boxplots[41] of monthly observed roadside dust lead concentrations (ppm) in each of the 3 domains. The urban burn scar is shown in red, the foothills region in gray, and urban Pasadena in blue, following the convention in Figure 1. Outliers in the Burn Scar region (3 points total) are removed for visualization.

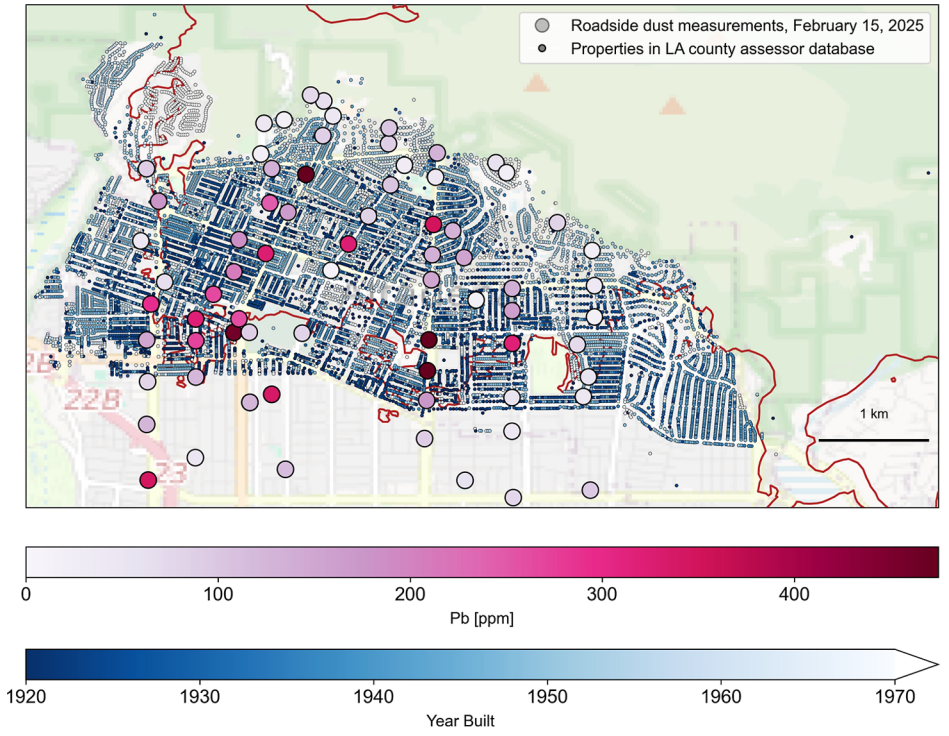

Figure 3. February 15th high-resolution spatial sampling of lead in roadside dust in red, plotted spatially with building construction date from the Los Angeles county assessors database in blue hues.[42] The red outline shows the fire perimeter.

RESULTS AND DISCUSSION

Lead in Roadside Dust

Dust collected in the immediate aftermath of the fires, near burned homes, contained notably high levels of lead (Figure 1). Once neighborhoods had been reopened to access by nonresidents, we collected samples of roadside dust from street gutters both inside the burn area and in nearby locations. This dust was sieved to obtain the fine fraction (<250 mm) and analyzed for total lead concentrations by X-ray fluorescence (XRF) spectrometry. Sampling locations were grouped into three main regions—within the Eaton fire urban burn scar (Burn Scar), a transect through urban Pasadena directly downwind of the urban fire (Urban Pasadena), and the remainder of samples along the mountain foothills outside of the burned area (Foothills) but still downwind of the wildland burn. Data for samples collected on February 1st, the first data on which samples were collected for all transect locations, highlights the spatial distribution of lead in Figure 1. In the Foothills locations, lead concentrations were typically below 100 ppm with a median concentration of 56 ppm. In Urban Pasadena locations, roadside dust lead concentrations were similarly low, with a median concentration of 83 ppm. Observed lead concentrations increased dramatically in the Burn Scar area, reaching up to 417 ppm with a median concentration of 240 ppm. This increase is sufficiently high that even under the known variability of the XRF technique (see Materials and Methods), we expect the larger-scale spatial differences to be robust.

https://doi.org/10.1021/acsestair.6c00015
ACS EST Air 2026, 3, 1789−1796

These locations were resampled seven times between January 26th and May 25th, over which time the amount of lead within the urban burn scar decreased back toward background levels (Figure 2). Median lead concentrations across the sample time period within the urban burn scar were 183 ppm, as compared to the lower 57.5 ppm along the foothills outside of the burn and 96 ppm in urban Pasadena. There is no significant trend over time in the median lead concentrations outside of the burn area for either the foothills (slope = −0.1 ppm/day, $p = 0.63$) or in urban Pasadena (slope = 0.04 ppm/day, $p = 0.93$) when fit with an interquartile-range-weighted ordinary least-squares regression. However, within the urban burn scar, where we expect additional lead inputs from the urban fire, there is a significant trend of −1.56 ppm/day ($p = 0.01$). The observed decrease in median concentrations begins between February and March, with a decrease of approximately 100 ppm, from a median of 250 ppm to 148 ppm. The median lead concentration in the burn scar decreased further to approximately 90 ppm and remained relatively stable in the following two months.

In principle, roadside dust in this area could come from a wide variety of sources, including not only ash and residue from burned buildings but also local traffic, soil and vegetation, transport and deposition of material from runoff, and deposition of atmospheric aerosol.[12−14] The very elevated lead concentrations within the urban burn scar relative to the locations outside provide strong evidence that the destroyed structures are a dominant source of lead in the dust. This is further supported by the median year buildings in this area were constructed, 1945—a time when lead was still routinely used in paint and plumbing.[15] Our measurements in Urban Pasadena and the Foothills are consistent with prior literature on lead in roadside dust, which shows that concentrations can be elevated above typical crustal rock, but are generally below 200 ppm.[12,13,16,17]

The supposition that lead from paint and other building materials in urban structures was the primary source of lead in roadside dust is further supported by a high-resolution sampling of roadside dust from February 15th (Figure 3). Within the burned area of Altadena, there is a pattern of older houses toward the center of Altadena, in the south. Toward the northern end of the burned area, the housing stock is generally more recent and was largely built during the 1950s through the 1970s. This pattern is reflected in the lead concentrations measured in roadside dust, with most samples containing less than 100 ppm lead, while higher lead concentrations are much more prevalent in toward the southern portion of the urban burn scar. This is overall consistent with these observations of elevated lead in roadside dust reflecting nearby burned structures.

The lead measurements shown here are higher than those from other well-studied fires at the wildland−urban interface. Following the 2021 Marshall fire in Colorado, there was limited evidence of lead concentrations in soils reaching the levels observed following the Eaton fire.[18,19] This is consistent with the difference in building age between the Marshall fire (median construction year of 1986) and buildings in Altadena (median year of 1945),[15] reinforcing the likely source of lead being older construction.

Lead in Atmospheric Aerosol

The dominant pathway by which the fires could impact lead concentrations in regions outside of the burn scar is through atmospheric transport and deposition. The low concentration of lead these regions is consistent with the time series of lead in atmospheric particulate matter (Figure 4). Smoke from the

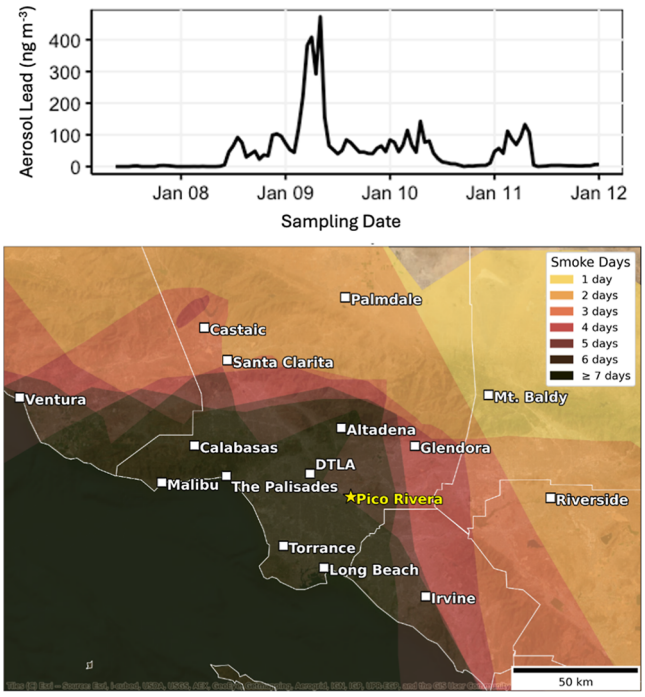

Figure 4. Top panel shows a reproduced time series of aerosol $PM_{2.5}$ lead concentrations as measured at the ASCENT Pico Rivera site (the yellow star in the left panel) in January 2025.[22] The bottom panel shows the spatial distribution of days with smoke over the greater Los Angeles region in January 2025.

January 2025 fires covered much of the greater Los Angeles region. Satellite-estimated smoke extents show the number of days in January 2025 when a smoke plume was identified from the NOAA Hazard Mapping System (HMS) smoke plume data.[20] In general, most of Southern California had at least 1 day with smoke overhead, and regions downwind of the Eaton firestorm (and the other LA fires) had upward of a week of smoky days. Similar to other major urban fire events, this smoke contained considerable lead concentrations for at least a portion of the time that burning occurred.[21,22] Previously published measurements of lead in particulate matter with a diameter less than 2.5 μm ($PM_{2.5}$) from the Atmospheric Science and Chemistry Network (ASCENT) are plotted in Figure 4 from January 7th through January 12th.[22] This site, located in Pico Rivera (shown as a yellow star in Figure 4), has been operational since July 2023 and reports hourly lead $PM_{2.5}$ concentrations. Lead in $PM_{2.5}$ was low (near 0) outside of a four-day window (Jan 8th−Jan 11th) when concentrations increased to approximately 100 ng/m^3, with a peak of nearly 500 ng/m^3.

Considerable ash deposition was reported downwind of the fire throughout Los Angeles.[23] However, the reasonably short increase of lead in $PM_{2.5}$—along with relatively high winds diluting the transported ash—helps explain why elevated lead concentrations in roadside dust were kept fairly local to the burned area and were not very elevated in dust downwind in Pasadena.

The relatively brief window of elevated lead concentrations, despite the large number of smoke days, can be at least

https://doi.org/10.1021/acsestair.6c00015
ACS EST Air 2026, 3, 1789−1796

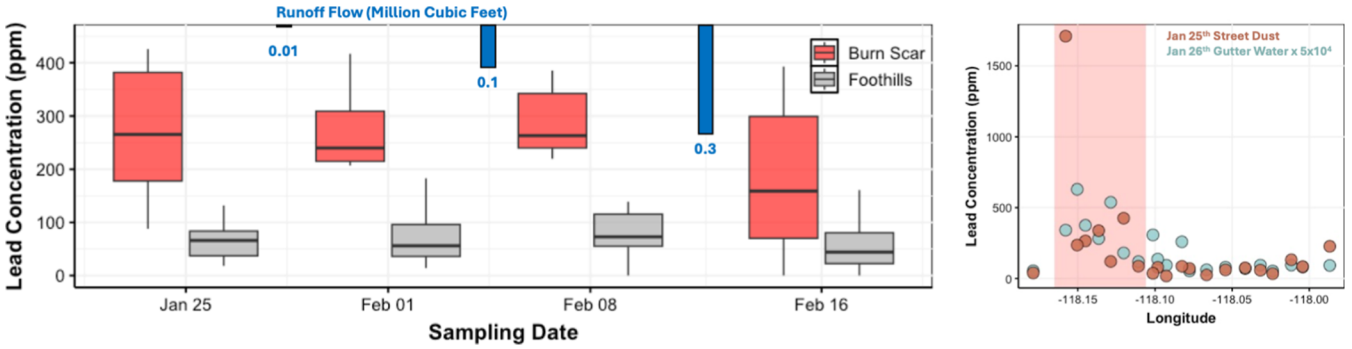

Figure 5. Boxplots[41] of observed roadside dust lead concentrations (ppm) in the Foothills and Burn Scar domains from January 25th through Feb 16th (left). The urban burn scar is shown in red and the foothills region in gray, following the convention in Figure 1. Outliers in the Burn Scar region (3 points total) are removed for visualization. Blue bars show the cumulative runoff flow in Eaton Wash between roadside dust observations. Gutter water samples from January 26th alongside street dust from January 25th are shown on the right as a function of longitude, where the red shaded region denotes the urban burn scar.

partially explained by two factors. First, the source of smoke changed as the fire moved through urban structures to burning vegetation in the nearby mountain wildlands—this change in fire fuel modifies the aerosol and ash composition.[9,21,24] Second, the HMS smoke plume data do not provide information regarding the vertical structure of the plume—smoke may be detected above a region, but the smoke can be high aloft and may not reach a sensor at the surface[25]—or, correspondingly, may not end up deposited on the surface.

Impacts of Rainfall on Environmental Lead

The decreasing roadside dust lead concentration in the burn scar was likely driven by several concomitant major rainfalls. In the month following the Eaton fire, there were three main rainfall events impacting the burn scar area.[26] The first and smallest rain event started on January 26th and accumulated an average of 0.6 in. across the urban burn region, followed by a series of scattered rainfall events throughout the week that began on February 6th, which accumulated a total of 2.5 in. of rain, and then the largest and most intense rain event in this time frame which began on February 13th and accumulated an average of 3.5 in. Runoff from these events was measured at the Eaton Wash, a site representative of the scale of runoff throughout the Eaton Canyon fire burn.[26] As is typical in Southern California, runoff increased nonlinearly with rainfall from 5632 to 117,589 to 301,840 cubic feet for the January 26th, February 6th, and February 13th rain events, respectively (Figure 5).

In between each of these rain events, we sampled the roadside dust across the transects shown in Figure 1 and measured lead concentrations, shown as a time series in Figure 5 for the Foothills and Burn Scar locations. The first two rain events did not appreciably change lead concentrations in the urban burn scar. However, the largest and most intense rain and runoff flow on February 13th was followed by the substantial 100 ppm decrease in lead that is apparent in Figure 2. This is consistent with the highly nonlinear threshold-based sediment transport process by which stormwater removes roadside dust—significant rainfall in a short period of time leads to powerful streams which wash out old sediment and wash in new sediment. Throughout the Foothills locations, there was not a statistically significant trend in roadside dust lead, consistent with both our assumption that these sites reflect the urban background lead concentrations in the area and the larger trends present in Figure 2.

Following the first rainfall event on January 26th, we sampled stormwater runoff in the same locations as the northern transect in Figure 1 (i.e., Burn Scar and Foothills sites), by collecting from puddles of standing or slowly flowing water as close as possible to the original sampling site, within roughly 2 h of the end of rainfall. Samples were filtered (0.2 mm), acidified, and analyzed for lead concentrations by ICPMS. Inside the burn scar, average lead concentrations in water were 7.0 ± 1.4 ppb (1s SD), while outside of the burn scar, average lead concentrations were 2.2 ± 0.4 ppb (Figure 5). The individual sites with the highest dust lead were not necessarily those with the highest rainwater lead, though both rainwater and dust showed the same overall pattern of elevated Pb within the urban burn scar (positive correlation; $R = 0.32$). We would not necessarily expect a direct relationship between lead concentrations in the runoff and dust at each specific sampling site, as the runoff represents a different catchment area than the equivalent catchment for transported dust and may be variably impacted by dilution.

Long-Term Outlook and Public Health Impacts

These high observed lead concentrations in roadside dust, atmospheric aerosol, and runoff could pose a potential health risk, particularly for more vulnerable populations such as children, people who are pregnant, and those with chronic health conditions. Soil with lead concentrations above 80 ppm can cause elevated blood lead levels and a potential decrease in children's IQ exceeding 1 point.[27,28] Nearly all of the urban burn scar dust meets this criterion (even considering potential variability in XRF measurements), as do most of the other dust samples. Indeed, lead concentrations above this threshold are ubiquitous in urban environments like Los Angeles and are a known public health concern.[29,30] The burned area roadside dust concentrations are all significantly higher than 80 ppm, closer to the observed ranges found in other notable urban lead disasters (e.g., greater than 250 ppm), including the Exide facility lead poisoning in Vernon, CA,[7] and urban lead concentrations following natural disasters like Hurricane Katrina[31,32] and Hurricane Sandy.[33] Additionally, the runoff concentrations of lead are in line with other studies that show increased concentrations following fires at the wildland–urban interface.[34−36] Atmospheric lead concentrations were generally well below what would be necessary to meet unhealthy levels.[22] However, these health concentration definitions are based on rolling three month average lead concentrations, and

https://doi.org/10.1021/acsestair.6c00015
ACS EST Air 2026, 3, 1789−1796

the short spike in atmospheric lead did not last long enough to meaningfully raise that longer-term average.[1,5] Detailed health assessments of acute exposure to elevated environmental lead concentrations are limited, and as such the full human health impact of this exposure event remains uncertain.

From a policy perspective, the lead levels in the stormwater runoff and atmospheric aerosol were generally below regulatory thresholds. However, many of the roadside dust samples collected were well above both the EPA threshold for soils of 200 ppm[29] and the California state threshold of 80 ppm.[27] In particular, nearly all of the roadside dust measurements in the burn scar prior to April 2025 met the criteria for cleanup for both federal and state lead levels, further motivating ongoing remediation efforts in the region. Moreover, it is likely that other contaminants besides lead were emitted during the fires.[9] Additional work investigating the concentration distributions of those contaminants will be informative for an environmental quality assessment.

Current remediation procedures focus on removing contaminated soil in only a portion of the Eaton Canyon fire burn area, centered on the footprint of burned structures.[37] Our sampling strategy focused on the material outside of this footprint (i.e., street gutters) and measured highly elevated lead concentrations. Roadside dust is more readily removed by rainfall, wind, and municipal cleanup (e.g., street sweeping) than dust on properties off the street. We posit that the measurements here are likely an upper bound on how rapidly lead may be removed from the urban environment following this fire—even if lead in roadside dust has decreased, it does not guarantee decreased lead in nearby properties. Our work therefore supports continued efforts to map the distribution of environmental lead contamination from the Eaton Canyon fires on individual properties and community spaces, both within the burned areas and in nearby neighborhoods.

■ ASSOCIATED CONTENT

Data Availability Statement

Bulk data and code are available here: https://doi.org/10.5281/zenodo.20740305.

Supporting Information

The Supporting Information is available free of charge at https://pubs.acs.org/doi/10.1021/acsestair.6c00015.

Figure S1 (DOCX)

■ AUTHOR INFORMATION

Corresponding Author

Sam J. Silva − *Department of Earth Sciences, University of Southern California, Los Angeles, California 90089, United States; Department of Civil and Environmental Engineering and Department of Population and Public Health Sciences, University of Southern California, Los Angeles, California 90089, United States;* orcid.org/0000-0001-6343-8382; Email: samsilva@usc.edu

Authors

Seth G. John − *Department of Earth Sciences, University of Southern California, Los Angeles, California 90089, United States*

A. Joshua West − *Department of Earth Sciences, University of Southern California, Los Angeles, California 90089, United States*

Mia Bradshaw − *Department of Biological Sciences, University of Southern California, Los Angeles, California 90089, United States*

Yadan Hu − *Department of Earth Sciences, University of Southern California, Los Angeles, California 90089, United States; State Key Laboratory of Loess Science, Institute of Earth Environment, Chinese Academy of Sciences, Xi'an 710061, China*

Cecilia M. John − *Department of Earth Sciences, University of Southern California, Los Angeles, California 90089, United States*

Kyeong Pil Kong − *Department of Earth Sciences, University of Southern California, Los Angeles, California 90089, United States*

Catherine Odendahl − *Department of Earth Sciences, University of Southern California, Los Angeles, California 90089, United States*

Nataly Pineda − *Department of Earth Sciences, University of Southern California, Los Angeles, California 90089, United States*

Adam Ross − *Department of Earth Sciences, University of Southern California, Los Angeles, California 90089, United States*

Brian Schlaff − *Department of Earth Sciences, University of Southern California, Los Angeles, California 90089, United States*

Nismata Sigdel − *Department of Earth Sciences, University of Southern California, Los Angeles, California 90089, United States*

Katherine Thomas − *Department of Biological Sciences, University of Southern California, Los Angeles, California 90089, United States*

Complete contact information is available at: https://pubs.acs.org/10.1021/acsestair.6c00015

Author Contributions

Conceptualization: S.G.J., S.J.S., and A.J.W. Investigation: S.J.S., S.G.J., A.J.W., M.B., Y.H., C.M.J., K.P.K., C.O., N.P., A.R., B.S., N.S., and K.T. Writing—original draft: S.J.S., S.G.J., and AJ.W. Writing—review and editing: S.J.S., SG.J., A.J.W., M.B., Y.H., C.M.J., K.P.K., C.O., N.P., A.R., B.S., N.S., and K.T.

Funding

This study was supported in part by a gift from FireAid Fund and by funding from the Wrigley Institute for Environmental Science (to S.G.J., J.S., and S.S.) and Simons Foundation award LI-SIAME-00001532 to S.G.J.

Notes

The authors declare no competing financial interest.

■ ACKNOWLEDGMENTS

The authors would like to thank the following people for assistance in sampling: O. J. Silva, R. A. Silva, D. G. Silva, B. E. Silva, and C. G. John.

■ REFERENCES

(1) Lanphear, B. P.; Rauch, S.; Auinger, P.; Allen, R. W.; Hornung, R. W. Low-Level Lead Exposure and Mortality in US Adults: A Population-Based Cohort Study. *Lancet Public Health* **2018**, *3* (4), e177−e184.

(2) Needleman, H. Lead Poisoning. *Annu. Rev. Med.* **2004**, *55* (1), 209−222.

(3) Lanphear, B.; Navas-Acien, A.; Bellinger, D. C. Lead Poisoning. *N. Engl. J. Med.* **2024**, *391* (17), 1621−1631.
(4) Hernberg, S. Lead Poisoning in a Historical Perspective. *Am. J. Ind. Med.* **2000**, *38* (3), 244−254.
(5) McFarland, M. J.; Hauer, M. E.; Reuben, A. Half of US Population Exposed to Adverse Lead Levels in Early Childhood. *Proc. Natl. Acad. Sci. U.S.A.* **2022**, *119* (11), No. e2118631119.
(6) Hanna-Attisha, M.; LaChance, J.; Sadler, R. C.; Champney Schnepp, A. Elevated Blood Lead Levels in Children Associated With the Flint Drinking Water Crisis: A Spatial Analysis of Risk and Public Health Response. *Am. J. Public Health* **2016**, *106* (2), 283−290.
(7) Johnston, J. E.; Hricko, A. Industrial Lead Poisoning in Los Angeles: Anatomy of a Public Health Failure. *Environ. Justice* **2017**, *10* (5), 162−167.
(8) Fisher, L. Environmental Law, Policy and Economics: Reclaiming the Environmental Agenda. By NICHOLAS ASHFORD and CHARLES CALDART. *J. Environ. Law* **2009**, *21* (2), 380−382.
(9) Holder, A. L.; Ahmed, A.; Vukovich, J. M.; Rao, V. Hazardous Air Pollutant Emissions Estimates from Wildfires in the Wildland Urban Interface. *PNAS Nexus* **2023**, *2* (6), pgad186.
(10) Eaton Fire|CAL FIRE. https://www.fire.ca.gov/incidents/2025/1/7/eaton-fire (accessed March 20, 2025).
(11) Qiu, M.; Chen, D.; Kelp, M.; Li, J.; Huang, G.; Yazdi, M. D. The Rising Threats of Wildland-Urban Interface Fires in the Era of Climate Change: The Los Angeles 2025 Fires. *Innovation* **2025**, *6*, 100835.
(12) Pan, H. A Comprehensive Analysis of Heavy Metals in Urban Road Dust of Xi'an, China: Contamination, Source Apportionment and Spatial Distribution. *Sci. Total Environ.* **2017**, *609*, 1361.
(13) Deocampo, D. M.; Reed, P. J.; Kalenuik, A. P. Road Dust Lead (Pb) in Two Neighborhoods of Urban Atlanta, (GA, USA). *Int. J. Environ. Res. Public Health* **2012**, *9*, 2020.
(14) Kauhaniemi, M.; Stojiljkovic, A.; Pirjola, L.; Karppinen, A.; Härkönen, J.; Kupiainen, K.; Kangas, L.; Aarnio, M. A.; Omstedt, G.; Denby, B. R.; Kukkonen, J. Comparison of the Predictions of Two Road Dust Emission Models with the Measurements of a Mobile Van. *Atmos. Chem. Phys.* **2014**, *14* (17), 9155−9169.
(15) B25035: Median Year Structure Built - Census Bureau Table. https://data.census.gov/table/ACSDT5Y2023.B25035?g=040XX00US06_160XX00US0601290&tid=ACSDT5Y2023.B25035 (accessed April 14, 2025).
(16) Bisht, L. Heavy Metal Concentration and Its Distribution Analysis in Urban Road Dust: A Case Study from Most Populated City of Indian State of Uttarakhand. *Spat. Spatiotemporal. Epidemiol.* **2022**, *40*, 100470.
(17) Świetlik, R.; Strzelecka, M.; Trojanowska, M. Evaluation of Traffic-Related Heavy Metals Emissions Using Noise Barrier Road Dust Analysis. *Spat. Pol. J. Environ. Stud.* **2013**, *22*, 561.
(18) Jech, S.; Adamchak, C.; Stokes, S. C.; Wiltse, M. E.; Callen, J.; VanderRoest, J.; Kelly, E. F.; Hinckley, E.-L. S.; Stein, H. J.; Borch, T.; Fierer, N. Determination of Soil Contamination at the Wildland-Urban Interface after the 2021 Marshall Fire in Colorado, USA. *Environ. Sci. Technol.* **2024**, *58*, 4326.
(19) Villarruel, C. M.; Figueroa, L. A.; Ranville, J. F. Quantification of Bioaccessible and Environmentally Relevant Trace Metals in Structure Ash from a Wildland−Urban Interface Fire. *Environ. Sci. Technol.* **2024**, *58* (5), 2502−2513.
(20) Office of Satellite and Product Operations, National Oceanic and Atmospheric Administration. Hazard Mapping System (HMS) Fire and Smoke Analysis, 2025. https://www.ospo.noaa.gov/products/land/hms.html#data (accessed Feb 01, 2025).
(21) Boaggio, K.; LeDuc, S. D.; Rice, R. B.; Duffney, P. F.; Foley, K. M.; Holder, A. L.; McDow, S.; Weaver, C. P. Beyond Particulate Matter Mass: Heightened Levels of Lead and Other Pollutants Associated with Destructive Fire Events in California. *Environ. Sci. Technol.* **2022**, *56* (20), 14272−14283.
(22) Baliaka, H. D.; Ward, R. X.; Bahreini, R.; Dillner, A. M.; Russell, A. G.; Seinfeld, J. H.; Flagan, R. C.; Wennberg, P. O.; Ng, N. L. Notes from the Field: Elevated Atmospheric Lead Levels During the Los Angeles Urban Fires-California, January 2025. *MMWR Morb. Mortal. Wkly. Rep.* **2025**, *74* (5), 69−71.
(23) What's in the smoke and ash of L.A.-area fires? County issues health warning, Los Angeles Times. https://www.latimes.com/california/story/2025-01-14/what-threats-lurk-in-the-smoke-and-ash-of-l-a-area-fires (accessed April 02, 2025).
(24) Akagi, S. K.; Yokelson, R. J.; Wiedinmyer, C.; Alvarado, M. J.; Reid, J. S.; Karl, T.; Crounse, J. D.; Wennberg, P. O. Emission Factors for Open and Domestic Biomass Burning for Use in Atmospheric Models. *Atmos. Chem. Phys.* **2011**, *11* (9), 4039−4072.
(25) Liu, T.; Panday, F. M.; Caine, M. C.; Kelp, M.; Pendergrass, D. C.; Mickley, L. J.; Ellicott, E. A.; Marlier, M. E.; Ahmadov, R.; James, E. P. Is the Smoke Aloft? Caveats Regarding the Use of the Hazard Mapping System (HMS) Smoke Product as a Proxy for Surface Smoke Presence across the United States. *Int. J. Wildland Fire* **2024**, *33*, WF23148.
(26) Rainfall. https://dpw.lacounty.gov/wrd/rainfall/ (accessed March 20, 2025).
(27) California Department of Toxic Substances Control. HUMAN HEALTH RISK ASSESSMENT (HHRA) NOTE NUMBER 3, DTSC-Modified Screening Levels (DTSC-SLs). https://dtsc.ca.gov/wp-content/uploads/sites/31/2022/02/HHRA-Note-3-June2020-Revised-May2022A.pdf (accessed April 02, 2025).
(28) California, S. of. LeadSpread-9. Department of Toxic Substances Control. https://dtsc.ca.gov/leadspread-9/ (accessed April 02, 2025).
(29) Filippelli, G. M.; Dietrich, M.; Shukle, J.; Wood, L.; Margenot, A.; Egendorf, S. P.; Mielke, H. W. One in Four US Households Likely Exceed New Soil Lead Guidance Levels. *GeoHealth* **2024**, *8* (6), No. e2024GH001045.
(30) Hung, W.-C.; Hernandez-Cira, M.; Jimenez, K.; Elston, I.; Jay, J. A. Preliminary Assessment of Lead Concentrations in Topsoil of 100 Parks in Los Angeles, California. *Appl. Geochem.* **2018**, *99*, 13−21.
(31) Rabito, F. A.; Iqbal, S.; Perry, S.; Arroyave, W.; Rice, J. C. Environmental Lead after Hurricane Katrina: Implications for Future Populations. *Environ. Health Perspect.* **2012**, *120* (2), 180−184.
(32) Zahran, S.; Mielke, H. W.; Gonzales, C. R.; Powell, E. T.; Weiler, S. New Orleans before and after Hurricanes Katrina/Rita: A Quasi-Experiment of the Association between Soil Lead and Children's Blood Lead. *Environ. Sci. Technol.* **2010**, *44* (12), 4433−4440.
(33) Mandigo, A. C.; DiScenza, D. J.; Keimowitz, A. R.; Fitzgerald, N. Chemical Contamination of Soils in the New York City Area Following Hurricane Sandy. *Environ. Geochem. Health* **2016**, *38* (5), 1115−1124.
(34) Stein, E. D.; Brown, J. S.; Hogue, T. S.; Burke, M. P.; Kinoshita, A. Stormwater Contaminant Loading Following Southern California Wildfires. *Environ. Toxicol. Chem.* **2012**, *31* (11), 2625−2638.
(35) Magliozzi, L. J.; Matiasek, S. J.; Alpers, C. N.; Korak, J. A.; McKnight, D.; Foster, A. L.; Ryan, J. N.; Roth, D. A.; Ku, P.; Tsui, M. T.-K.; Chow, A. T.; Webster, J. P. Wildland−Urban Interface Wildfire Increases Metal Contributions to Stormwater Runoff in Paradise, California. *Environ. Sci.: Processes Impacts* **2024**, *26* (4), 667−685.
(36) Pinedo-Gonzalez, P.; Hellige, B.; West, A. J.; Sañudo-Wilhelmy, S. A. Changes in the Size Partitioning of Metals in Storm Runoff Following Wildfires: Implications for the Transport of Bioactive Trace Metals. *Appl. Geochem.* **2017**, *83*, 62−71.
(37) Key Facts & Frequently Requested Info. https://www.spl.usace.army.mil/Missions/Emergency-Management/Los-Angeles-County-Wildfire-Debris-Removal-Mission/Key-Facts-Frequently-Requested-Info/ (accessed April 01, 2025).
(38) Clos, H.; Chrysochoou, M. Optimizing pXRF Sample Preparation for in Situ Soil Screening: A Regulatory Framework Perspective. *J. Environ. Qual.* **2025**, *54*, 1128−1140.
(39) Jenkins, E.; Galbraith, J.; Paltseva, A. Portable X-Ray Fluorescence as a Tool for Urban Soil Contamination Analysis: Accuracy, Precision, and Practicality. *EGUsphere* **2024**, *2004*, 1.
(40) Al Maliki, A.; Al-lami, A. K.; Hussain, H. M.; Al-Ansari, N. Comparison between Inductively Coupled Plasma and X-Ray

https://doi.org/10.1021/acsestair.6c00015
ACS EST Air 2026, 3, 1789−1796

Fluorescence Performance for Pb Analysis in Environmental Soil Samples. *Environ. Earth Sci.* **2017**, *76* (12), 433.
(41) Wickham, H. *Ggplot2: Elegant Graphics for Data Analysis*; Springer-Verlag: New York, 2016.
(42) Assessor Parcel Data (Rolls 2021 - Present). https://data.lacounty.gov/datasets/lacounty::assessor-parcel-data-rolls-2021-present/explore (accessed June 27, 2025).

https://doi.org/10.1021/acsestair.6c00015
ACS EST Air 2026, 3, 1789−1796